# Flow Visualisation inside a Flip-Flop using UVP

Jiro FUNAKI, Katsuya HIRATA, Tatsuya INOUE and Hiroyuki MATSUDA
Dept. Mech. Engng., Doshisha Univ., Kyoto 610-0321, Japan
Hirochika TANIGAWA
Dept. Mech. Engng., Maizuru Tech., Maizuru 625-8511, Japan

This research deals with the switching mechanism of a flip-flop jet nozzle with a connecting tube, which is based on the measurements of pressure in two chambers, velocity in the connecting tube and velocity distribution between two inside walls of the nozzle, *i.e.*, reattachment walls. The authors particularly focus on the details of switching flow field inside the nozzle, using a Ultrasound-Velocity-Profile monitor (UVP monitor). As a result, two re-circulating flows, *viz*., two vortical structures, are shown on both side walls inside the nozzle. By means of the simultaneous observation of chamber pressures and connecting-tube velocity with UVP results, we show a coherent scenario of this jet-oscillation phenomenon.

**Keywords:** Flowmeter, Fluid Logic, Fluidics, UVP, UDM, Flow Induced Vibration

## 1 INTRODUCTION

The flip-flop jet nozzle (hereafter, referred to as FFJN) is one of the oscillator elements of the fluid logic, which uses the Coanda effect where a jet reattaches to a side wall. (for example, see[1]).The FFJN has control ports on both side walls near a primary nozzle. Two chambers connected to the control port are linked by a connecting tube, to cause jet's oscillation. From the practical points of view, we can use the FFJN as a flow meters, because its oscillation frequency increases with flow rate. In addition, the FFJN is useful for shear-layer control and mixing enhancement with secondary flow. For example, Morris et al.[2] have considered the application to gas-solid two phase flow, and showed the mixing enhancement as fuel-spray nozzles. In general, as the FFJN has no mechanically moving parts, it keeps good features such as low production cost, high reliability and robustness against temperature variation density variation and so on.

References [2]-[6] are best studies about the FFJN. Raman et al.[5] has conducted experiments on the nozzle with various geometries, and shown the relation of the oscillation frequency with the connecting-tube length, with the connecting-tube volume and with the nozzle-pressure ratio. Funaki et al.[6] have shown that the jet's switching occurs when the time-integral of inflow momentum from the control port into the lower side attains a certain value. However, we have no knowledge about the detail of the flow inside the FFJN.

In the present study, in order to reveal the flow field inside the FFJN, we carry out the measurements on flow velocity distributions inside the FFJN, on pressures in the chambers and on velocity in the connecting tube. Because flow inside the FFJN is turbulent, we conduct a conditional sampling by ultrasound-velocity-profile monitor (hereafter, referred to as UVP), using a connecting tube velocity as a reference.

## NOMENCLATURE

| | |
|---|---|
| $b$ | : breadth of an primary-nozzle exit [m] |
| $d$ | : inner diameter of a connecting tube [m] |
| $f$ | : frequency of a oscillating jet [Hz] |
| $L$ | : length of a connecting tube [m] |
| $P_A$ | : pressure in Chamber A [Pa] |
| $P_B$ | : pressure in Chamber B [Pa] |
| $Q$ | : total flow rate [$m^3$/s] |
| $Q_A$ | : half section flow rate of the side A [$m^3$/s] |
| $t$ | : time [s] |
| $T$ | : period of a oscillation jet [1/s] |
| $U_{PN}$ | : velocity at a primary-nozzle exit [m/s] |
| $U_{CT}$ | : velocity at a connecting-tube section [m/s] |
| $R_A$ | : reattachment length on the side A [m] |
| $R_B$ | : reattachment length on the side B [m] |
| $\zeta$ | : vorticity [$s^{-1}$] |
| * | : non-dimensional |

## 2 EXPERIMENTAL METHOD

Fig.1 shows a schematic diagram of the tested FFJN. We decide its basic geometrical dimensions according to Viet's[3]. (For the details, see Tab.1.) Here we take the breadth *b* of an primary-nozzle exit as a length scale, and the mean flow velocity at the primary-nozzle exit as a velocity scale. Tested Reynolds number is fixed to $1.83 \times 10^4$.

Fig.2 shows a schematic diagram of the present experimental apparatus. A turbo pump ① drives the flow of water from a large water tank. Through a flow meter ② and a long straight pipe ③ as a flow conditioner, water flows into a FFJN ④. As the

FFJN is sunk in the large water tank, water can circulates.

We measure velocities inside the FFJN and a connecting tube ⑤ using a UVP monitor system ⑥ and ⑦. we measure pressures in two chambers are using pressure transducer ⑧ with a strain amplifier ⑨. Data from the UVP monitor and the pressure transducers are simultaneously recorded by a PC ⑩ with a A/D-converter board.

Fig.3 shows the position of a ultrasound transducer for the inside FFJN measurement with the present coordinate system. We traverse the transducer in the *y* direction (cross-streamwise) with a spatial resolution of 0.15s, or in the *x* direction (streamwise) with a spatial resolution of 0.22s.

The transducer's oscillation frequency is 4[MHz]. UVP measurement volume is a disc with a diameter of 5[mm] and with a thickness of 0.75[mm].

The transfer particles are made of polyethylene with a mean diameter of $1.2\times10^{4}$[m]. As the Specific gravity of the tracer particles is 0.918, we coat them with detergent in order to avoid them, floating on water surfaces.

Fig.4 (a) shows a sample raw of the velocities inside the FFJN. In general, the flow inside the FFJN is periodical, but it include strong turbulent components. For simultaneous, the number of available UVP transducers is limited. Therefore, it is necessary to conduct a conditional sampling to only periodic components. Here, we take the pressure difference $\Delta P$ between two chambers, as a reference signal. Specifically speaking, as shown in Fig.4 (b), we divide one period *T* into eight, equivalently. Then, at the times of these eight points, we assembly average raw velocities over 50 periods.

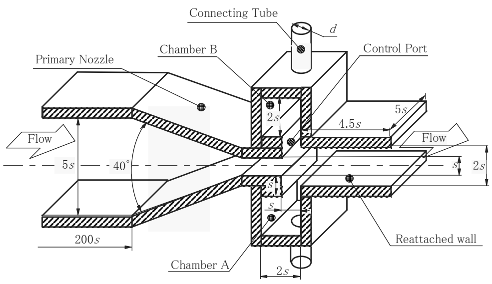


Fig. 1: Schematic of flip-flop jet nozzle.

Tab. 1: Experimental parameters.

| | |
|---|---|
| *s* [m] | 0.04 |
| *h* [m] | 0.2 |
| *AR* (=*h/s*) | 5 |
| *d* [m] | 0.052 |
| *d/s* | 1.3 |
| *L* [m] | 1.6 |
| *L/s* | 40 |
| *Re* | $1.83\times10^{4}$ |

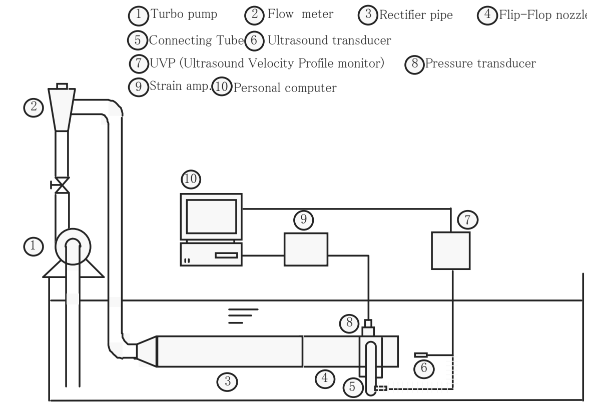


Fig. 2: Schematic of experimental apparatus.

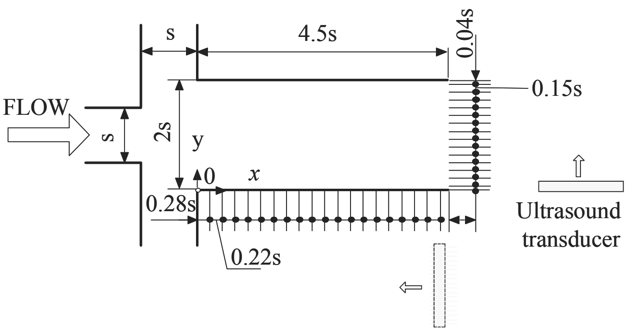


Fig. 3: Position of Ultrasound transducer and coordinate system.

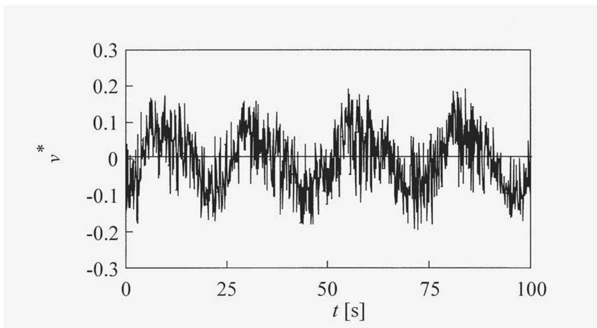


(a)$v^{*}$(*x/s*=3.83, *y/s*=1.00)

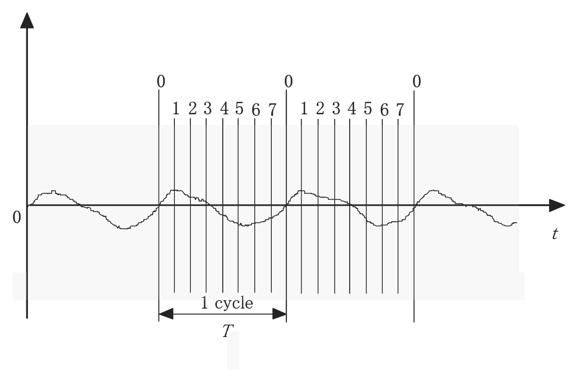


(b) $\Delta P$ and sampling-point definition

Fig. 4: Sampling raw data.

## 3 RESULTS AND DISCUSSION

### *3.1 Velocity vectors and vorticity contours inside the FFJN*

Fig.5 shows velocity vectors and vorticity contours inside the FFJN with no oscillation. Here, to cease flow oscillation, we close the control parts. The jet from the primary nozzle defects toward the side A, which is the lower side in the figure. Usually, the primary-nozzle jet keeps to deflect toward either the side A or the side B. And we can make the jet deflect toward the side B by means of appropriate initial disturbances.

We compare the no-oscillation jet in Fig.5, with the most deflected jet in Fig.6 (g) and Fig.7 (g). At first, we focus on re-circulating flow on the upper side B. The re-circulating flow in Fig.5 (a) is slightly longer than that in Fig.6 (g). While it is difficult to read the magnitude of the reverse-flow velocity from the figures, the magnitude in Fig.5 (a) tends to be much longer than Fig.6 (g). The magnitudes of vorticity in the reverse-flow in Fig.5 (b) are almost same as Fig.7 (g). But, the maximum-magnitude location, which is approximated to be the re-circulating-flow centre, in Fig.5 (b) is closer to the side wall B than Fig.7 (g).

Next, we show the jet in ordinary oscillation. Fig.6 and 7 show timely-successive velocity vectors and vorticity contours in one period, respectively. We can confirm exactly periodic oscillator flow in both figures. We can also confirm the close correspondence between Fig.6 and 7.

When we watch near side-wall areas, we can observe reverse flows on the both side walls at any time. Namely, a re-circulating flow always exists on each side wall.

Next, we focus on a re-circulating flow on the lower side A. There is no reverse flow, in Fig.5, while there is small but strong reverse flow in Fig.6 (g) and 7 (g). In Fig.5, a re-circulating-flow region becomes small enough to go out of the present visualized range.

In summary, the flow in ordinary oscillation jet is far from the corresponding non-oscillation flow.

### *3.2 Relation of inside FFJN flow with connecting –tube flow*

Fig.8 show assembly-averaged time histories of the connecting-tube flow parameters and the inside-FFJN flow parameters. Specifically speaking, as the former, we show the pressures $P_A$ and $P_B$ in the chamber A and B, the difference $\Delta P$ between $P_A$ and $P_B$, and the non-dimensional velocity $U_{CT}^*$ at a connecting-tube cross section. As the latter, we show the non-dimensional reattachment lengths $R_A$ and $R_B$ on the side A and B, the non-dimensional vorticities $\zeta_A^*$ and $\zeta_B^*$ at upstream points on the side A and B at $(x/s, y/s)$=(0.50,0.67) and (0.50,1.67), and the non-dimensional half-section flow rate $Q_A/Q$ on the side A. Here, $U_{TU}^*$ is positive, when the flow in the connecting tube goes from the side A to the side B, and vice versa. We can confirm almost synchronized relations among $P_A$, $P_B$, $\Delta P$, $R_A^*$, $R_B^*$, $\zeta_A^*$ and $\zeta_B^*$, but there are a slight phase lag in $Q_A/Q$ and large phase lag in $U_{TU}^*$ in comparison with those.

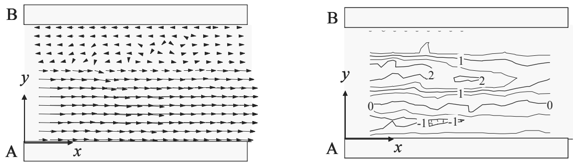


(a) Velocity vectors (b) Vorticity contours

Fig. 5: Flow of non-oscillating jet.

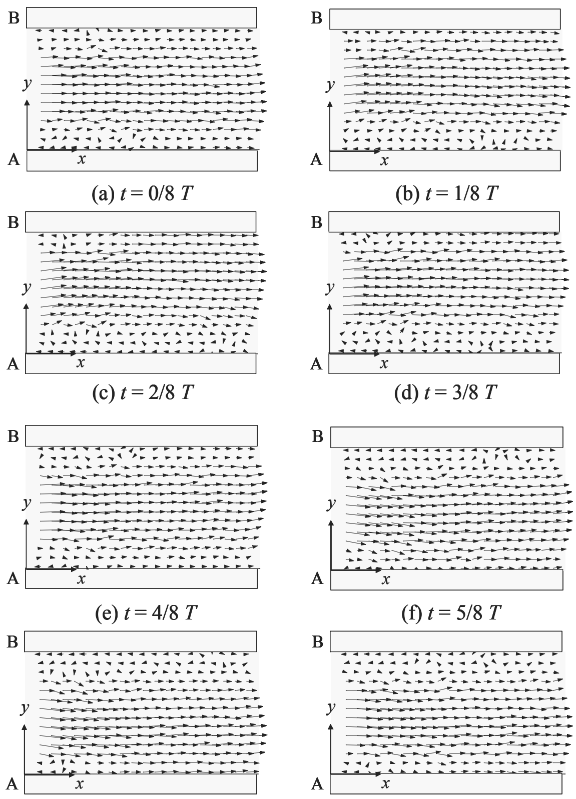


(a) $t$ = 0/8 $T$ (b) $t$ = 1/8 $T$

(c) $t$ = 2/8 $T$ (d) $t$ = 3/8 $T$

(e) $t$ = 4/8 $T$ (f) $t$ = 5/8 $T$

(g) $t$ = 6/8 $T$ (h) $t$ = 7/8 $T$

Fig. 6: A sequence of velocity vectors in a period.

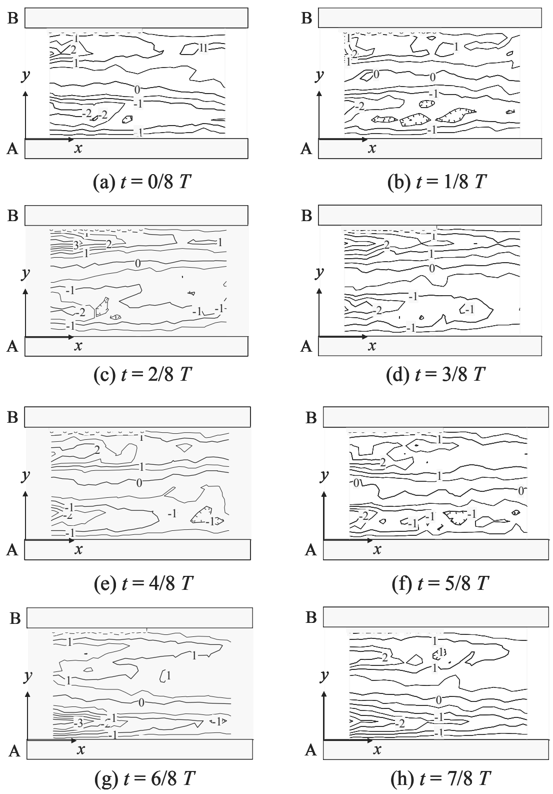


Fig. 7: A sequence of vorticity contours in a period.

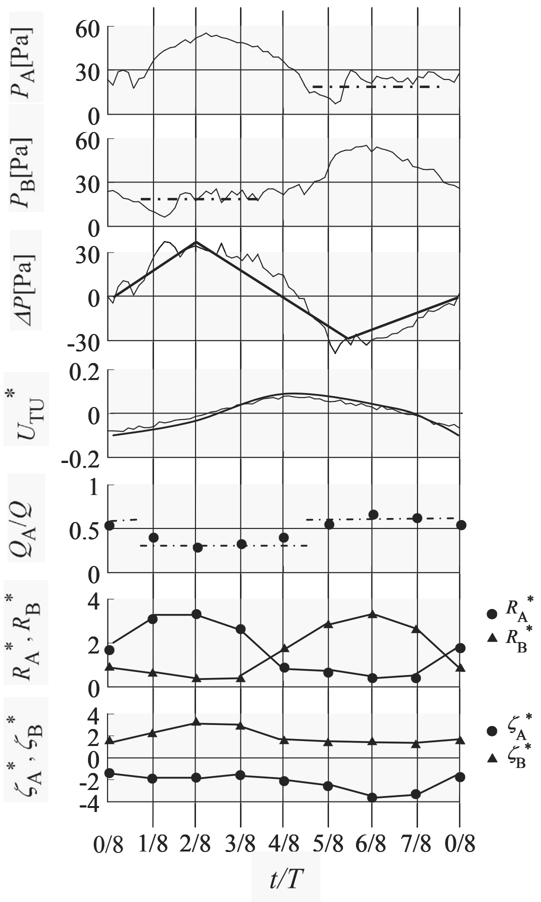


Fig. 8: Time history of $P_A$, $P_B$, $\triangle P$, $U_{TU}$, and $Q_A/Q$ in a period.

## ACKNOWLEDGEMENTS

This study was partly supported by the Academic Frontier Research Project on "Next Generation Zero-emission Energy Conversion System" of Ministry of Education, Culture, Sports, Science and Technology.

## 4 CONCLUSIONS

In order to reveal the oscillation phenomenon is the FFJN, we have conducted UVP measurements using a conditional sampling technique. Non-oscillating flow is far from the flow in ordinary oscillation. At any time, there is a re-circulating flow, which is accompanied with a flow re-attachment and with reverse flow. We have shown timely-consecutive velocity vectors and vorticity contours in one period. In addition, by means of simultaneous measurements for a connecting tube, we have shown the relation between the inside flow and the connecting tube flow.

## REFERENCES

[1]Ozaki, S. and Hara, Y., Introduction to Fluid Logic, Nikkan-Kyoto-Shinbunsha, Tokyo, 1963.

[2]Morris, G.J., Jurewicz, J.T. and Palmer, G.M., "Gas-Solid Flow in a Fluidically Oscillating Jet," *Trans. ASME Journal of Fluids Engineering*, Vol.114, 1992, pp. 362-366.

[3]Viets, H., "Flip-Flop Jet Nozzle," *AIAA Journal,* Vol.13, No.10, 1975, pp. 1375-1379.

[4]Raman, G., Hailye, M. and Rice, E. J., "Flip-Flop Jet Nozzle Extended to Supersonic Flows," *AIAA Journal,* Vol.31, No.6, 1993, pp. 1028-1035.

[5]Raman, G., Rice, E. J., Cornelius, D. M., "Evaluation of Flip-Flop Jet Nozzle for Use as Practical Excitation Davices," *Trans. ASME,* Vol.116, 1994, pp.508-515.

[6]Funaki, J., Mizuno, Go., Kondo, M. and Hirata K., "Oscillation Mechanism of a Flip-Flop Jet Nozzle Based on the Flow which Flows through a Connecting Tube," *Trans. JSME(Series B)*, Vol.65, No.631, 1999, pp. 928-933 (in Japanese).

[7]Rockwell, D. and Naudascher, E., "self-Sustained Oscillations of Impinging Free Shear Layers," *Ann. Rev. Fluid Mech.*, Vol.11, 1979, pp. 67-94.